Spectrally Efficient WDM Nyquist Pulse-Shaped Subcarrier Modulation Using a Dual-Drive Mach–Zehnder Modulator and Direct Detection

M. Sezer Erkılınç, *Student Member, IEEE*, Manoj P. Thakur, *Member, IEEE*, Stephan Pachnicke, *Senior Member, IEEE*, Helmut Griesser, *Member, IEEE*, John Mitchell, *Senior Member, IEEE*, Benn C. Thomsen, *Member, IEEE*, Polina Bayvel, *Fellow, IEEE*, and Robert I. Killey, *Member, IEEE*

***Abstract*—High data transmission capacity is increasingly needed in short- and medium-haul optical communication links. Cost-effective wavelength division multiplexed (WDM) transceiver architectures, achieving high information spectral densities (ISDs) (>1 b/s/Hz) and using low-complexity direct detection receivers are attractive solutions for such links. In this paper, we assess the use of dual-drive Mach–Zehnder modulators (DD-MZMs), and compare them with in-phase quadrature (*IQ*)-modulators for generating spectrally-efficient single sideband Nyquist pulse-shaped 16-QAM subcarrier (N-SCM) modulation format signals. The impact of the extinction ratio (ER) of a modulator on the optical sideband suppression ratio (OSSR) was investigated for the SSB signals in WDM systems, together with the resulting impact on inter-channel crosstalk penalties. First, in back-to-back operation, an *IQ*-modulator with an ER of 30 dB and a DD-MZM with an ER of 18 dB were experimentally compared in a 6×25 Gb/s WDM system by varying the channel spacing. Following this comparison, 16 GHz-spaced 6×25 Gb/s WDM signal transmission was experimentally demonstrated using the DD-MZM. The experiment was performed using a recirculating loop with uncompensated standard single-mode fiber (SSMF) and EDFA-only amplification. The maximum achievable transmission distances for single channel and WDM signals were found to be 565 and 242 km, respectively, at a net optical ISD of 1.5 b/s/Hz. This is the first experimental comparison of such modulator types for SSB N-SCM signal generation and the highest achieved ISD using a DD-MZM in direct-detection WDM transmission.**

***Index Terms*—Direct detection, dual-drive MZM, electronic predistortion, ISD, Nyquist pulse shaping, optical fiber communication, SSB, subcarrier modulation, WDM.**

Manuscript received June 2, 2015; revised September 7, 2015; accepted October 19, 2015. Date of publication November 4, 2015; date of current version February 10, 2016. This work was supported by the EU ERA-NET+ project PIANO+ IMPACT, EPSRC UNLOC EP/J017582/1, and EU FP7 project ASTRON.

M. S. Erkılınç, B. C. Thomsen, P. Bayvel, and R. I. Killey are with the Optical Networks Group, Department of Electronic and Electrical Engineering, University College London, London WC1E 7JE, U.K. (e-mail: m.erkilinc@ee.ucl.ac.uk; b.thomsen@ucl.ac.uk; p.bayvel@ucl.ac.uk; r.killey@ucl.ac.uk).

M. P. Thakur and J. Mitchell are with the Communications and Information Systems Group, Department of Electronic and Electrical Engineering, University College London, London WC1E 7JE, U.K. (e-mail: manoj.thakur@ucl.ac.uk; j.mitchell@ucl.ac.uk).

S. Pachnicke is at the ADVA Optical Networking SE, Maerzenquelle 1-3, 98617 Meiningen, Germany (e-mail: spachnicke@advaoptical.com).

H. Griesser is at the ADVA Optical Networking SE, Fraunhoferstr. 9a, 82152 Martinsried, Germany (e-mail: hgriesser@advaoptical.com).

Color versions of one or more of the figures in this paper are available online at http://ieeexplore.ieee.org.

Digital Object Identifier 10.1109/JLT.2015.2497343

I. Introduction

SPECTRALLY-EFFICIENT modulation schemes achieving information spectral densities (ISDs) greater than 1 b/s/Hz using direct detection receivers are attractive for access, metropolitan, and regional links due to their simplicity and low-cost. In such links, the cost-effectiveness is the primary requirement coupled with low power consumption. To achieve this, the optical complexity of the transceiver architecture needs to be minimized using low-cost and low-complexity optical components. Although the highest channel bit rates and ISDs are achievable using coherent receivers with polarization multiplexing [1]–[3], direct detection receiver-based solutions, i.e., using a single-ended photodiode with no delay interferometer(s) and a single analogue-to-digital converter (ADC), are potentially preferable for metro networks since such receivers significantly reduce the costs. Network operators are installing 100 Gb/s solutions, comprising four dense wavelength division multiplexed (DWDM) channels carrying 28 Gb/s per wavelength, to support data transmission over metro distances [4].

To achieve ISDs greater than 1 b/s/Hz at low-cost, multi-level modulation schemes, such as 16-*ary* quadrature amplitude modulation (16-QAM) or higher, and electronic equalization can be implemented through the use of digital signal processing (DSP)-based transceivers. It is expected that the use of high sampling rate digital-to-analogue converters (DACs) and ADCs will be acceptable in future low-cost systems, as the performance of silicon complementary metal oxide semiconductor technology continues to increase, whereas the cost and power consumption reduce. Therefore, to reduce the cost, each transmitter should employ a simple modulator with a high linewidth laser (typically ≥1 MHz) and a simple receiver consisting of a single-ended photodiode. Amongst the formats offering high ISD (>1 b/s/Hz) and good dispersion tolerance (>100 km), dispersion pre-compensated single sideband (SSB) Nyquist pulse-shaped subcarrier modulation (N-SCM) has been shown to be one of the strongest candidates [5]–[10].

An optical SSB signal can be generated using either an intensity modulator combined with an optical sideband filter [11] or a dual input optical modulator, such as an in-phase quadrature (*IQ*)-modulator [7]–[10], [12] or a dual-drive Mach–Zehnder modulator (DD-MZM) [13]–[16]. If one of the sidebands is partially suppressed, it is referred to as vestigial sideband signalling [17]. Compared to the *IQ*-modulator, the DD-MZM has

a simpler structure and a smaller footprint, and offers lower optical loss.

In the work described in this paper, a performance comparison between an *IQ*-modulator and a DD-MZM in a spectrally-efficient WDM system was carried out. The system operated at a net bit rate of 24 Gb/s per channel (a gross bit rate of 25 Gb/s), taking into account the hard-decision forward error correction (HD-FEC) overhead. The impact of the extinction ratio (ER) on the optical sideband suppression ratio (OSSR), that affects the inter-channel crosstalk, limiting the channel spacing, and consequently, the achievable spectral efficiency, was assessed in simulations and experimentally. The WDM channel spacing was varied from 12 to 20 GHz (net optical ISDs from 2 to 1.2 b/s/Hz) for the ER values of 10–40 dB. Note that such (non-conventional) channel spacing values are chosen in order to maximize the ISD with the available DACs, RF-amplifiers and modulators.

Following the back-to-back comparison, a study on the use of DD-MZMs for spectrally-efficient WDM (16 GHz-spaced 6×25 Gb/s) SSB Nyquist pulse-shaped 16-QAM SCM signal transmission, yielding a net optical ISD of 1.5 b/s/Hz, was carried out. The chromatic dispersion accumulated along the fiber link was compensated using electronic pre-distortion (EPD) [18]–[20]. All the channels were successfully transmitted over 242 km of uncompensated standard single-mode fiber (SSMF), achieving a bit-error ratio (BER) of below 3.8×10^{-3}, taken as the HD-FEC threshold.

II. Review of Optical SSB Signal Generation Using IQ-Modulators and DD-MZMs

In this section, the principle of operation of the *IQ*-modulator and DD-MZM are briefly discussed. We highlight the impact of the ER of the modulator on the OSSR in the generation of optical SSB signals in DWDM systems at ISDs greater than 1 b/s/Hz.

A DD-MZM, sometimes referred to as dual-electrode MZM or polar modulator, consists of two phase modulators, driven by two independent electrical signals (V_1 and V_2) [21]. The input optical field ($E_{\rm in}$) is split into two arms and phase modulation is applied to both arms. Then, the phase-modulated optical fields are coupled to generate the output optical field ($E_{\rm out}$). If the insertion loss of the MZM is ignored, the DD-MZM input–output relationship is given by

$$E_{\rm out} = E_{\rm in}\left[\gamma \exp\left(j\pi\frac{(V_1+V_{\rm dc})}{V_\pi}\right) + (1-\gamma)\exp\left(j\pi\frac{V_2}{V_\pi}\right)\right], \tag{1}$$

where γ is the optical splitting ratio with a value between 0 and 1. V_π is the differential voltage between the two electrodes to provide a π phase-shift between the two waveguides, and $V_{\rm dc}$ is the applied dc bias voltage. Note that the terminal for V_2 is assumed to be grounded. Having two independent phase modulators enables to generate two phase-modulated signals. These signals can be used to implement arbitrary amplitude and phase modulation, such as high-order QAM signalling. However, the driving signals (V_1 and V_2) need to be correctly mapped from Cartesian to polar coordinates as described in [22], [23].

An *IQ*-modulator consists of two intensity modulators (typically two single-drive MZMs) and a phase shifter. The $E_{\rm in}$ is split into two paths, the *I* and *Q* arms. The optical field amplitude modulation is achieved by biasing the single-drive MZMs at their minimum transmission (null) point ($V_{I\rm dc} = V_{Q\rm dc} = 0$). With a relative $\pi/2$ phase-difference induced by the phase modulator, the $E_{\rm out}$ can realize any constellation point(s) on the complex *IQ*-plane (in Cartesian coordinates) after the outputs of the two arms are coupled. The $E_{\rm out}$ can be defined as

$$E_{\rm out} = E_{\rm in}\left[\gamma\cos\left(\frac{V_I+V_{I\rm dc}}{V_\pi}\pi\right) + j(1-\gamma)\cos\left(\frac{V_Q+V_{Q\rm dc}}{V_\pi}\pi\right)\right], \tag{2}$$

where V_I and V_Q are the electrical driving signals.

To generate an optical SSB signal using a dual-input optical (vector) modulator, such as a DD-MZM or an *IQ*-modulator, the two independent arms need to be driven such that the unwanted sideband from each arm of the modulator interfere destructively, while the desired ones interfere constructively. Therefore, the time dependent driving signals, V_1 and V_2, are

$$V_1 = \frac{V_{1_{\rm rms}}}{V_\pi}[x_r(t) - \hat{x}_i(t)] \quad \text{and} \quad V_2 = \frac{V_{2_{\rm rms}}}{V_\pi}[\hat{x}_r(t) + x_i(t)], \tag{3}$$

where $x_r(t)$ and $x_i(t)$ are the real and imaginary parts of a time dependent signal, $\hat{x}_r(t)$ and $\hat{x}_i(t)$ are their Hilbert transforms, and $V_{1_{\rm rms}}$ and $V_{2_{\rm rms}}$ are the root mean square (RMS) value of the driving signals, respectively. The Hilbert transform is a process in which all negative frequency components of a signal are phase-advanced by 90° whereas all positive frequency components are phase-delayed by 90°. The amplitude of the spectrum remains unchanged. In other words, it introduces a 180° phase difference between the negative and positive frequency components of an input signal [24]–[26]. If the electrical signal $x(t)$ is real-valued, $x_i(t)$ and $\hat{x}_i(t)$ become zero. Otherwise, a butterfly structure needs to be used, e.g., if the signal is pre-distorted/dispersed to mitigate the chromatic dispersion. In the case of the DD-MZM, the signal waveforms generated in Cartesian coordinates need to be converted to polar coordinates using Eq. (6) and Eq. (7) in [22]. Note that in all cases, the attenuations and the phase of the driving signals should be controlled identically to obtain maximum sideband suppression.

The ER of an optical modulator is crucial in the generation of an optical SSB signal. If the $E_{\rm in}$ is not equally split, the unwanted sideband is not fully suppressed, causing a spectral broadening. Hence, linear crosstalk between the neighbouring WDM channels is observed (assuming no optical filtering is used when the WDM channels are combined, e.g., if it is carried out with an optical coupler), and consequently, it causes penalties at channel spacing values of less than twice the SSB signal bandwidth. The ER of an optical modulator, which is related to

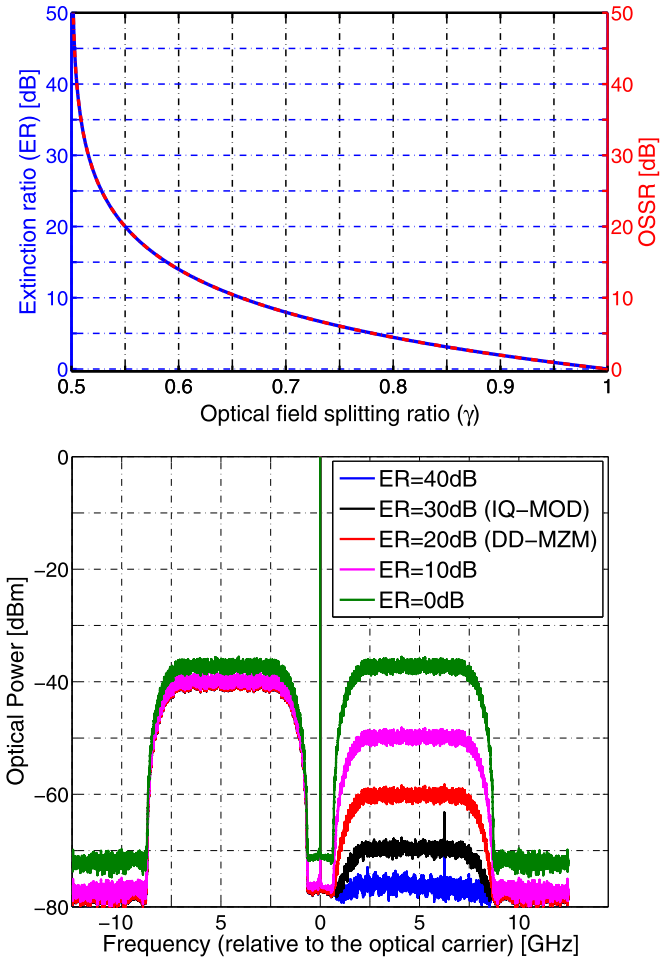

Fig. 1. ER and OSSR with respect to γ of the optical modulator (top). Simulated optical spectra at a resolution of 10 MHz for different ER values (bottom).

γ, is given by

$$\mathrm{ER(dB)} = -20\log_{10}|2\gamma - 1| \approx \mathrm{OSSR(dB)}. \tag{4}$$

Moreover, if the SSB signal is generated utilizing the Hilbert transform, the OSSR, defined as the power of the desired sideband divided by the power of the suppressed sideband, is approximately equal to the ER, assuming the attenuation and the phase on both arms are optimized. The change in OSSR and ER with respect to γ are shown in Fig. 1 along with the simulated optical spectra at certain ER values. For instance, if the incoming light is split with a ratio of 0.55 ($0.55E_{\mathrm{in}}$ to one arm and $0.45E_{\mathrm{in}}$ to the other arm), the ER of the modulator is 20 dB, meaning that the unwanted sideband can be suppressed by up to approximately 20 dB, as can be seen in Fig. 1.

III. Numerical Simulations and Experimental Setup

In this section, the simulation model for the Nyquist pulse-shaped SCM signal generation, transmission and detection along with the (offline) experimental waveform generation is described in detail. Then, the experimental setup is outlined.

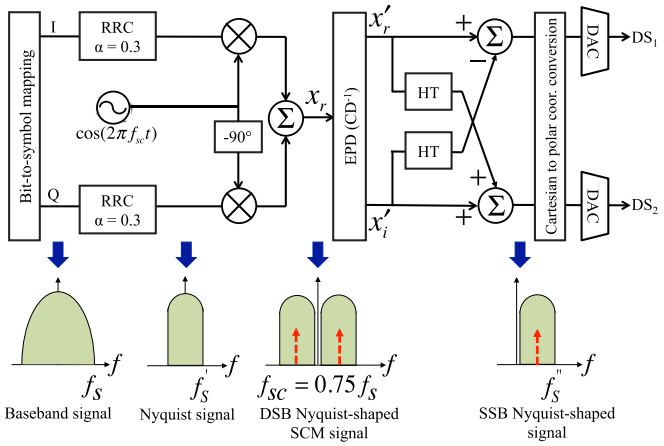

Fig. 2. Block diagram of Nyquist-SCM transmitter DSP (top) and the schematic of the signal spectra of DSB and SSB three quarter-cycle ($f_{sc} = 0.75f_s$) Nyquist pulse-shaped ($\alpha = 0.3$) SCM (bottom). x_r: real-valued DSB Nyquist-SCM signal. $x'r(t)$ and $x'i(t)$: real and imaginary parts of the pre-dispersed SSB Nyquist-SCM signal. f_s: symbol rate, f_{sc}: subcarrier frequency, $f_s^{'} = f_s/2(1+\alpha)$, $f_s^{''} = f_{sc} + f_s^{'}$, EPD: Electronic pre-distortion and CD: Chromatic dispersion.

A. Numerical Simulations and Offline Waveform Generation

The simulation model for the Nyquist pulse-shaped 16-QAM SCM signal generation, transmission and detection was implemented in MATLAB. Four 2^{18} patterns, based on de Bruijn bit sequences and decorrelated by 0.25 of the pattern length, were mapped to 16-QAM symbols at a symbol rate (f_s) of 6.25 GBd. After bit-to-symbol mapping, a pair of root raised-cosine (RRC) pulse-shaping filters with a roll-off factor (α) of 0.3, 256 taps and a stop-band attenuation of 40 dB were applied to the *I*- and *Q*-baseband signals. The baseband signals were up-converted to a subcarrier frequency (f_{sc}) of 4.68 GHz ($0.75\times f_s$) and added to each other to generate a real-valued DSB Nyquist pulse-shaped SCM signal, denoted as $x_r(t)$, at a bit rate of 25 Gb/s, as shown in Fig. 2. Dispersion pre-compensation was implemented by applying the inverse of the transfer function of the fiber (neglecting loss and nonlinearity) to mitigate the dispersion, as described in [18]–[20]. Finally, two 6-bit quantized pre-dispersed signals, $\mathrm{DS}_1 = x_r(t) - \hat{x}_i(t)$ and $\mathrm{DS}_2 = \hat{x}_r(t) + x_i(t)$, were used to achieve SSB signalling, as shown in Fig. 2. Cartesian to polar coordinate conversion was performed when using a DD-MZM, as given by Eq. (6) and Eq. (7) in [22].

The effective number of bits (ENOB) of the DACs used in the experiment was measured to be 3.8 bits at 10 GHz. Therefore, in the simulations, the electrical signal-to-noise ratio of the driving signals was set to 23 dB to emulate the DAC quantization noise. The low-pass filters (LPFs) used in the experiment to remove the images generated by the DACs were modeled as fifth-order Bessel filters with a bandwidth of 7 GHz. The single channel SSB signal was generated using Eq. (1) for the DD-MZM with an ER of 18 dB ($\gamma = 0.56$) and Eq. (2) for the *IQ*-modulator with an ER of 30 dB ($\gamma = 0.51$), respectively. As the optical source, a distributed feedback (DFB) laser with a linewidth of 1 MHz was used, operating at 1550 nm. In WDM simulations, the channels carrying 25 Gb/s SSB Nyquist pulse-shaped

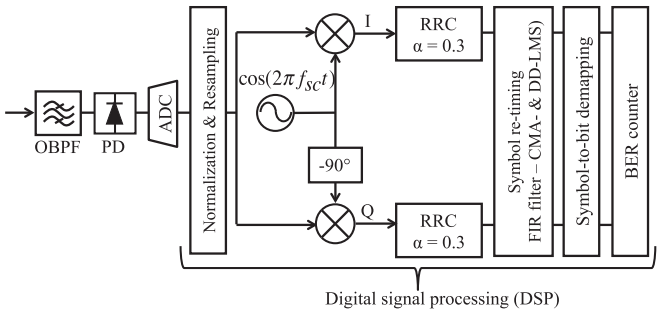

Fig. 3. Block diagram of Nyquist-SCM receiver. CMA: Constant modulus algorithm, DD: Decision-directed, LMS: Least mean squares and FIR: Finite-impulse response.

16-QAM SCM signal were decorrelated by approximately 1000 symbols.

The symmetric split-step Fourier method [27] was utilized to model the single channel and WDM signal transmission at a simulation bandwidth of 200 GHz with step sizes of 1 km and 400 m, respectively. The fiber parameters ($\alpha, D, \gamma_{\text{NL}}$ and L_{span}) were 0.2 dB/km, 17 ps/(nm.km), 1.2 $\text{W}^{-1} \cdot \text{km}^{-1}$ and 80 km, respectively. To emulate the nonlinear interaction between the signal and amplified spontaneous emission (ASE)-noise, all ASE-noise generated by the EDFAs was added inline.

Before photodetection using a single-ended photodiode with a responsivity of 0.8 A/W, a fourth-order super-Gaussian optical band-pass filter (OBPF) was applied to demultiplex the channel of interest and remove out-of-band ASE-noise. Following the resampling and quantization of the digitized signal by a single ADC with an ENOB of 5-bit at 10 GHz and a sampling rate of 50 GSa/s, a fifth-order Bessel LPF with a bandwidth of 16 GHz was used to emulate the frequency response of the real-time sampling scope used in the experiment. The block diagram of the receiver DSP is shown in Fig. 3. The resampled quantized signal was first split into two branches, and subsequently, down-converted to generate the *I*- and *Q*-baseband signals. A pair of matched RRC filters with $\alpha = 0.3$ were used, followed by a 5-tap FIR filter for symbol re-timing and the BER counter. Initially, the constant modulus algorithm was chosen as a cost function for fast convergence, and then, switched to decision directed least-mean squares (LMS). Finally, the BER was computed by error counting over 2^{20} bits. To calculate the upper bounds on the net bit rate and net optical ISD, the hard decision decoding bound for the binary symmetric channel was utilized resulting in a maximum code rate (r) of [28]:

$$r = 1 + p_b \log_2 p_b + (1 - p_b)\log_2(1 - p_b), \tag{5}$$

where p_b is the BER. Using Eq. (5), r was found to be 0.96 at a p_b of 3.8×10^{-3}, yielding a net bit rate of 24 Gb/s per channel (a gross bit rate of 25 Gb/s) and a net optical ISD of 1.5 b/s/Hz (a gross optical ISD of 1.56 Gb/s) in the WDM transmission. The simulation and experimental results are discussed together in Section IV.

B. Experimental Setup

The optical transmission test-bed used for the experiment consisted of a WDM SSB Nyquist pulse-shaped 16-QAM SCM transmitter, an optical fiber recirculating loop and a direct detection receiver, as shown in Fig. 4. As previously described in Section III-A, the driving signal waveforms for the modulators, "DS_1" and "DS_2," were generated offline in MATLAB using 2^{15} de Bruijn bit sequences, as shown in Fig. 2. The waveforms were quantized to 6 bits for the DACs (Micram VEGA DACII) with an ENOB of 3.8 bits at 10 GHz operating at a sampling rate of 25 GSa/s, and uploaded to the memory of a pair of Xilinx Virtex-5 FPGAs' RAM blocks. To prevent linear crosstalk between neighbouring channels due to the images generated by the DACs, electrical anti-imaging filters, fifth-order Bessel LPFs with a bandwidth of 7 GHz, were used. The LiNbO_3 *IQ*-modulator with a V_π of 3.5 V was driven by the electrical signals with a V_{pp} of 3.4 V whereas the V_{pp} of the driving signals was set to 2.4 V for the LiNbO_3 DD-MZM with a V_π of 2.6 V. The optical carrier was added by biasing the modulator (*IQ*-modulator or DD-MZM) close to its quadrature point to achieve approximately linear mapping from the electrical to the optical domain with the bias voltages adjusted to achieve the desired optical carrier-to-signal power ratio (CSPR). Note that the CSPR is defined as the ratio between the optical carrier and the sideband power. In the single channel case, only the DFB laser operating at λ_3 was used. The optical spectrum of the single channel taken from the optical spectrum analyser operating at a resolution bandwidth of 0.01 nm is shown in the inset (a) of Fig. 4.

In the WDM case, first, the channel spacing was varied from 12 to 20 GHz in back-to-back operation to assess the impact of the finite optical sideband suppression on the interchannel crosstalk penalty. DFB lasers ($\lambda_{1,3,5}$) with a linewidth of approximately 1 MHz at 1549.60 nm, separated by twice the channel spacing, were used as optical sources for both the *IQ*-modulator and DD-MZM. The odd channels ($\lambda_{1,3,5}$) were frequency shifted by the value of the channel spacing using a separate *IQ*-modulator. As shown in Fig. 4, both arms of this *IQ*-modulator were driven by a signal generator with a tone at the frequency corresponding to the WDM channel spacing. The phase shifters on both arms were adjusted such that a 90° phase difference was obtained between two arms to suppress one of the side tones by approximately 30 dB, and the modulator was biased at its null point to suppress the light at the original frequency. The odd channels were delayed using fiber of length 3.4 m length (a delay of 17 ns corresponding to 429 samples) to achieve signal decorrelation between odd and even channels. Finally, the odd and even channels were combined using a 3 dB coupler to generate the WDM SSB Nyquist pulse-shaped 16-QAM SCM signal, as illustrated in Fig. 4 with its optical spectrum, given in the inset (b). The optimum channel spacing was chosen based on the trade-off between maximizing the ISD and minimizing the required OSNR penalty caused by the linear crosstalk between neighbouring channels.

Once the optimum channel spacing was determined, the transmission experiment was performed using an optical

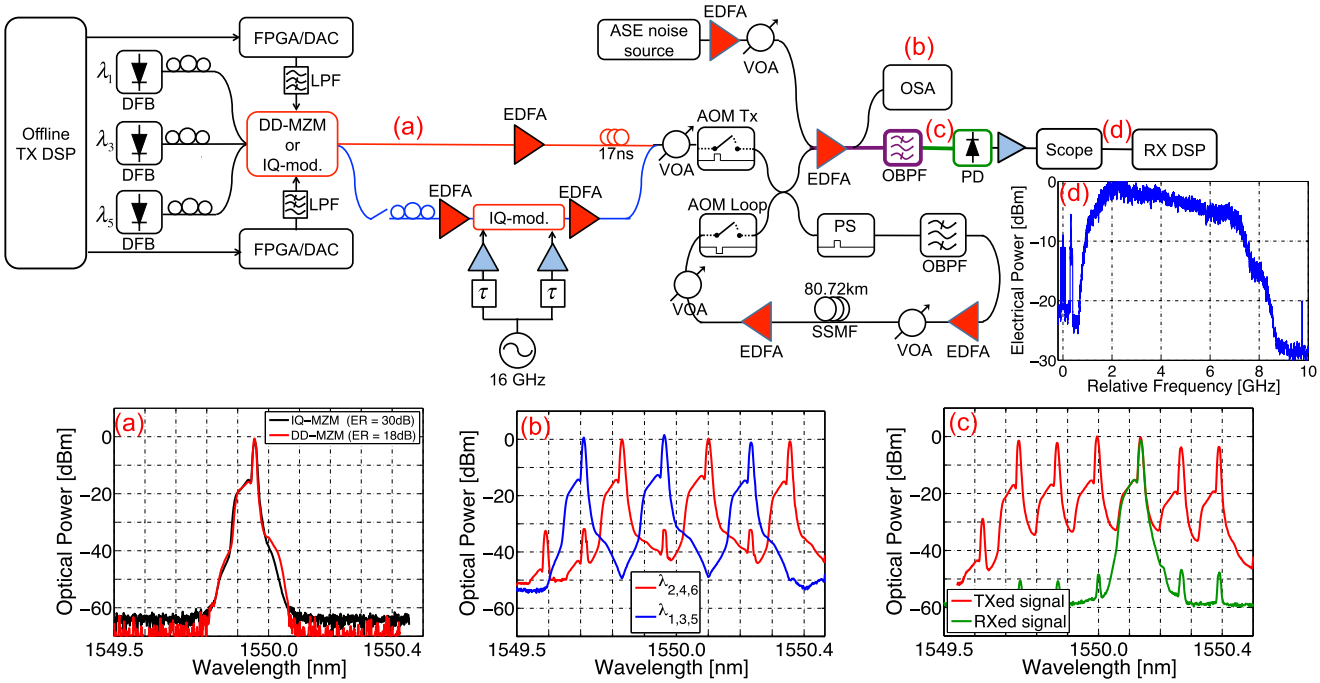

Fig. 4. Experimental setup for WDM SSB Nyquist pulse-shaped SCM transmission. FPGA: Field programmable gate array, VOA: Variable optical attenuator, AOM: Acousto-optic modulator, PS: Polarization scrambler, OBPF: Optical band-pass filter, PD: Photodiode. Insets: (a) Experimental optical spectrum of single channel generated using *IQ*- and DD-MZ modulators, (b) transmitted WDM signal with (c) the received optical spectrum. (d) Received electrical spectrum. Offline TX and RX DSP are shown in Figs. 2 and 3, respectively.

recirculating loop with a single span of 80.7 km SSMF, as shown in Fig. 4. The fiber parameters, D, α and γ_{NL} were 17 ps/nm/km, 0.2 dB/km and 1.2 $\text{W}^{-1}\cdot\text{km}^{-1}$, respectively. An OBPF (Yenista Optics XTM50-Wide) with a bandwidth of 200 GHz and a filter edge gradient of 500 dB/nm was used to filter the out-of-band ASE-noise during the transmission. A loop synchronous polarization scrambler (PS) was utilized to randomize the signal polarization state at each circulation. The launch power into the span was controlled by variable optical attenuators (VOAs). The fiber loss (16 dB) plus the insertion loss of the loop components (15 dB from VOAs, PS, AOM and OBPF) resulted in a total loss of 31 dB per recirculation. This loss was compensated by two EDFAs with a noise figure of 5 dB operating at their saturation point (18 dBm output power).

At the receiver, the channel of interest was demultiplexed using a manually tunable OBPF (Yenista Optics XTM50-Ultrafine) with a 3 dB bandwidth of 2 GHz less than the channel spacing and a filter edge gradient of 800 dB/nm, as shown in the inset (c) of Fig. 4. A single-ended PIN Discovery photodiode (DSC10H) was used to detect the filtered optical signal, followed by an RF-amplifier. The received electrical signal spectrum after digitization using a single ADC, operating at 50 GSa/s with an electrical bandwidth of 16 GHz and a nominal resolution of 8 bits (ENOB of 5 bits at 10 GHz), is shown in the inset (d) of Fig. 4. The receiver DSP used in the simulations, as described in Section III-A with the block diagram presented in Fig. 3, was also used in the experiments. The BER was computed by error counting over 2^{20} bits.

IV. Transmission Results and Discussions

In this section, the performance of the *IQ*-modulator and DD-MZM is compared for the single channel and WDM signals in back-to-back operation. In the WDM case, the channel spacing was varied from 12 to 20 GHz. The experimentally measured and simulated required OSNR values of the WDM SSB Nyquist pulse-shaped 16-QAM SCM signals are presented. Following the comparison, the single channel and WDM transmission results for the SSB Nyquist pulse-shaped 16-QAM SCM signal generated by the DD-MZM are presented in Section IV-B.

A. Back-to-Back Performance

The BER versus OSNR values for the single channel case, with the received constellations at an OSNR of 34 dB are shown in Fig. 5. Ideal system simulations were performed, neglecting any practical limitations such as DAC/ADC quantization noise, and non-ideal optical and electrical filtering effects. The required OSNR at the HD-FEC threshold in ideal simulations was found to be 21 dB at a BER of 3.8×10^{-3} for the SSB Nyquist pulse-shaped 16-QAM SCM signal with $\alpha = 0.3$ and $f_{\text{sc}} = 4.68$ GHz ($0.75 \times f_s$). In our experiment, the implementation penalty, as compared to the ideal system simulations, was found to be 2 dB (a required OSNR of 23 dB) caused by the DAC quantization noise, low-pass filtering effects and the non-ideal OBPF at the receiver before the photodiode. Moreover, there was no significant performance difference observed between the *IQ*-modulator and DD-MZM for the single channel case, as presented in Fig. 5.

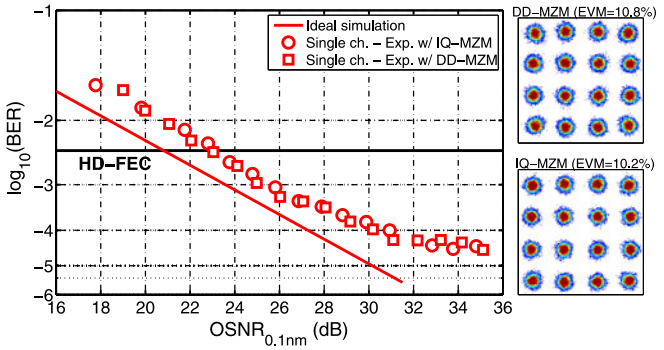

Fig. 5. Back-to-back BER versus OSNR values for the single channel case using the *IQ*-modulator and DD-MZM. The received constellations at an OSNR of 34 dB with an EVM of 10.2% and 10.8%. EVM is defined as the difference between the measured and ideal symbols, calculated as the RMS value, as given in Eq. (10) in [29].

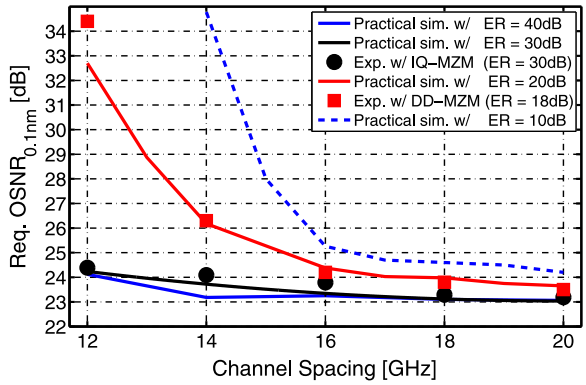

Fig. 6. Simulated and experimental required OSNR values with respect to the channel spacing using the *IQ*-modulator and DD-MZM.

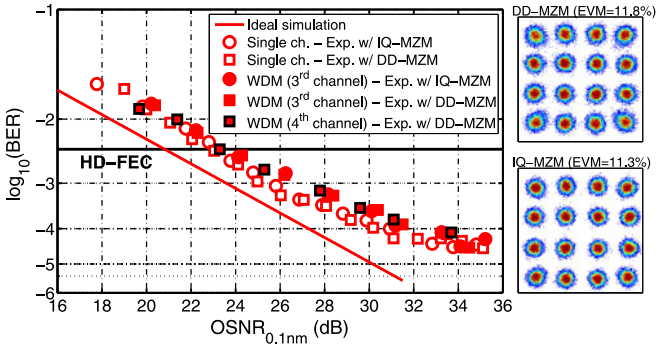

Fig. 7. BER versus OSNR for the WDM system using the *IQ*-modulator and DD-MZM (left). The received constellations at an OSNR of 34 dB (right).

After the single channel measurements, the channel spacing was varied from 12 to 20 GHz (a net optical ISD of from 2 to 1.2 b/s/Hz). Using the *IQ*-modulator and DD-MZM, the back-to-back required OSNR values for the WDM system were compared experimentally and in practical simulations using different values of the ER. The simulation setup is described in Section III-A. One of the central channels (λ_3) was selected as the channel of interest during these measurements. In the practical system simulations with an ER of 40 dB, no significant OSNR penalty was observed at channel spacing above 12 GHz. The OSNR penalty at a channel spacing of 12 GHz is due to the non-ideal demultiplexing before the photodiode. In the experiment, using the DD-MZM, the required OSNR values were found to be 34 and 26 dB (the OSNR penalties of 11 and 3 dB compared to the single channel case) at channel spacings of 12 and 14 GHz, respectively. The values for the *IQ*-modulator at the same channel spacings were measured to be 24.4 and 24.1 dB (OSNR penalties of 1.4 and 1.1 dB compared to the single channel case), respectively. The OSNR penalties observed in the DD-MZM case are due to the lower suppression of the unwanted sideband compared to the *IQ*-modulator, resulting in higher linear crosstalk between the neighbouring channels. The suppression ratio, typically limited to 20 dB for a DD-MZM, can be increased to 45 dB by cascading DD-MZM with a phase modulator, as experimentally demonstrated in [16]. At a channel spacing of 16 GHz or more, the measured required OSNR penalties were found to be within 1 dB compared to the single channel performance. The experimental results for the WDM system matched well with the practical simulation results, as can be seen in Fig. 6. As a result, we chose 16 GHz as the channel spacing value for the WDM transmission experiment using the DD-MZM, explained in Section IV-B. The optimum CSPR at the HD-FEC threshold was found to be approximately 9 dB for both single channel and WDM signals. The high CSPR is mainly due to the overlap between the sideband and the signal-signal beating terms, resulting in interference. In direct detection links, the optimum CSPR is dependent on the OSNR value. A detailed discussion regarding the optimum CSPR value can be found in [10]. It is worth noting that if the WDM transmission is realized using the *IQ*-modulator instead of the DD-MZM, the channel spacing can be chosen as 12 GHz, yielding an ISD of 2 b/s/Hz, as demonstrated in [10].

Once the optimum channel spacing was determined using the DD-MZM, the back-to-back BER versus OSNR performance for the 16 GHz-spaced WDM (6ch.$\times$25 Gb/s) SSB Nyquist pulse-shaped 16-QAM SCM signal generated by the *IQ*-modulator and DD-MZM was measured, and presented in Fig. 7 along with the received constellations at an OSNR of 34 dB. In the DD-MZM case, the BER values were measured both for the third (λ_3) and fourth (λ_4) channels. The frequency stability of the DFB lasers was approximately $\pm$2 GHz which is reasonable for low-cost direct detection links over metropolitan distances. Nevertheless, this does not cause any significant penalties ($<$0.5 dB) since the signal bandwidth is 8.75 GHz whereas the channel spacing is chosen as 16 GHz.

B. Transmission Performance

Following the back-to-back performance assessment, single channel and WDM signal transmission experiments were carried out using the recirculating fiber loop. The experimentally measured BER values with respect to the launch power per channel are shown in Fig. 8 including the received constellations at their optimum launch power values. The maximum achievable single channel transmission distance was 565 km and the optimum launch power was found to be 2 dBm, operating at an optimum CSPR of approximately 9 dB at the HD-FEC

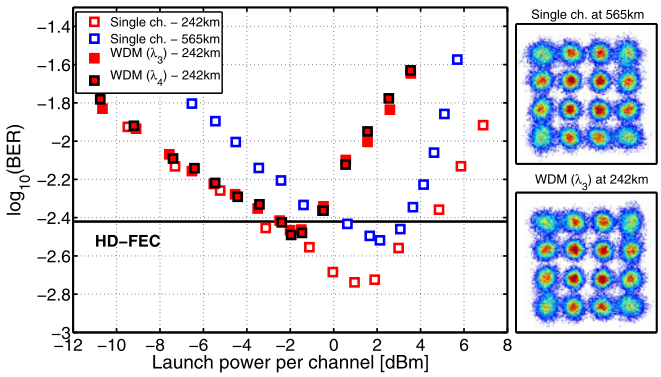

Fig. 8. BER versus launch power per channel for WDM transmission using DD-MZM (left). The received constellations at the optimum launch power (right).

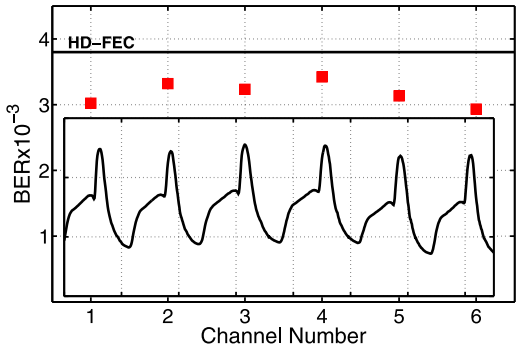

Fig. 9. The measured BER values for each received channel using DD-MZM at 242 km. Inset: Transmitted optical spectrum.

threshold, similar to the back-to-back operation. Since there is no significant penalty observed between the single channel and WDM back-to-back performance (see Fig. 7), the transmission performance at a given distance (242 km) is very similar in the linear regime, as can be observed in Fig. 8. However, the maximum achievable transmission distance was reduced from 565 to 242 km due to the additional inter-channel nonlinear effects during the WDM transmission. The optimum launch power per channel for the WDM signal was found to be -2 dBm, 4 dB less than the single channel transmission. The optimum CSPR value in WDM transmission was found to be approximately 7.5–8 dB at 242 km, slightly lower that for the single channel transmission at 565 km. This small change in the optimum CSPR value is due to the trade-off between the SSBI and fiber nonlinearities, and, as expected, the optimum CSPR value is lower in WDM transmission because of the fiber nonlinearities. The experimental BER values for WDM transmission were measured for both λ_3 and λ_4 channels after WDM transmission.

Furthermore, all six transmitted channels carrying the SSB Nyquist pulse-shaped 16-QAM SCM signal and operating at a bit rate of 25 Gb/s, generated by the DD-MZM, achieved a BER below 3.8×10^{-3} at the optimum launch power per channel, as shown in Fig. 9 with the transmitted optical spectrum. A net optical ISD of 1.5 b/s/Hz was achieved over 242 km of SSMF. This is the highest achieved ISD using a DD-MZM in direct detection links over this transmission distance. It is worth noting that the maximum achieved ISD in direct detection links is reported as 2 b/s/Hz at 343 km using an *IQ*-modulator [10].

V. Summary and Conclusion

We have investigated the generation of SSB N-SCM signals using *IQ*- and dual-drive MZ modulators, including the effect of the finite ER of the modulator in relation to the optical sideband suppression, and the resulting crosstalk between neighbouring WDM channels. To demonstrate this relationship, we compared, both in simulations and experimentally, the back-to-back performance of 25 Gb/s per channel WDM SSB Nyquist pulse-shaped 16-QAM SCM signaling using an *IQ*-modulator with an ER of 30 dB and a DD-MZM with an ER of 18 dB. At a channel spacing of 16 GHz or more, no significant differences in the required OSNR value were observed between the modulators at the HD-FEC threshold. In contrast, due to the lower optical sideband suppression, the required OSNR values increases by 2 and 10 dB using the DD-MZM compared to the *IQ*-modulator at channel spacings of 14 and 12 GHz, respectively.

Following this, we carried out WDM SSB Nyquist pulse-shaped 16-QAM SCM signal transmission experiments using the DD-MZM at a channel spacing of 16 GHz, achieving a net optical ISD of 1.5 b/s/Hz. The required OSNR values for the single channel and WDM signals were both found to be 23.2 dB due to the relatively large channel spacing. The maximum achievable transmission distance over EDFA-only amplified SSMF link, with 31 dB loss per amplifier span, was 565 km for the single channel, and decreasing to 242 km in the WDM case due to the inter-channel nonlinear effects. Finally, it was shown that all six transmitted channels achieved BER values below the HD-FEC threshold at the maximum WDM transmission distance of 242 km. To the best of our knowledge, this is the first experimental performance comparison of *IQ*-modulator and DD-MZM for SSB Nyquist pulse-shaped SCM signalling. Moreover, it is the highest achieved ISD, at this distance, among the reported experimental single polarization WDM demonstrations in direct detection links using a DD-MZM based transmitter and a direct detection receiver, comprising a single-ended photodiode with a single ADC. The experimental results indicate that the direct detection SSB Nyquist pulse-shaped SCM modulation technique using compact DD-MZMs can be a promising and practical approach for metro, regional and access applications. It offers a high ISD with a cost-effective transceiver design.

Acknowledgment

The authors would like to thank Dr. S. Mikroulis for providing the $LiNbO_3$ DD-MZM.

References

[1] M. Mazurczyk, "Spectral shaping in long haul optical coherent systems with high spectral efficiency," *J. Lightw. Technol.*, vol. 32, no. 16, pp. 2915–2924, Aug. 2014.
[2] J. X. Cai, "100 G transmission over transoceanic distance with high spectral efficiency and large capacity," *J. Lightw. Technol.*, vol. 30, no. 24, pp. 3845–3856, Dec. 2012.
[3] P. Winzer, "High spectral-efficiency optical modulation formats," *J. Lightw. Technol.*, vol. 30, no. 24, pp. 3824–3835, Dec. 2012.

[4] ADVA, *Efficient 100G Transport* (2014). (retrieved November 1st 2015). [Online]. Available: http://www.advaoptical.com/en/innovation/100g-transport/100g-metro.aspx

[5] A. S. Karar and J. C. Cartledge, "100 Gb/s intensity modulation and direct detection," *J. Lightw. Technol.*, vol. 32, no. 16, pp. 2809–2814, (invited paper) Aug. 2014.

[6] N. Liu, X. Chen, C. Ju, and R. Hui, "40-Gbps vestigial sideband half-cycle Nyquist subcarrier modulation transmission experiment and its comparison with orthogonal frequency division multiplexing," *Opt. Eng.*, vol. 53, no. 9, p. 096114, 2014.

[7] M. S. Erkilinc, R. Maher, M. Paskov, S. Kilmurray, S. Pachnicke, H. Griesser, B. C. Thomsen, P. Bayvel, and R. Killey, "Spectrally-efficient single-sideband subcarrier-multiplexed quasi-Nyquist QPSK with direct detection," presented at the European Conf. Exhibition Optical Commun., London, U.K., 2013, Paper Tu3C4.

[8] M. S. Erkılınç, S. Kilmurray, R. Maher, M. Paskov, R. Bouziane, S. Pachnicke, H. Griesser, B. C. Thomsen, P. Bayvel, and R. I. Killey, "Nyquist-shaped dispersion-precompensated subcarrier modulation with direct detection for spectrally-efficient WDM transmission," *Opt. Exp.*, vol. 22, no. 8, pp. 9420–9431, 2014.

[9] M.S. Erkılınç, S. Pachnicke, H. Griesser, B.C. Thomsen, P. Bayvel, and R. Killey, "Performance comparison of single sideband direct detection Nyquist-subcarrier modulation and OFDM," *J. Lightw. Technol.*, vol. 33, no. 10, pp. 2038–2046, May 2015.

[10] M. S. Erkılınç, Z. Li, S. Pachnicke, H. Griesser, B. C. Thomsen, P. Bayvel, and R. Killey, "Spectrally-efficient WDM Nyquist-pulse-shaped 16-QAM subcarrier modulation transmission with direct detection," *J. Lightw. Technol.*, vol. 33, no. 15, pp. 3147–3155, Aug. 2015.

[11] B. J. C. Schmidt, A. J. Lowery, and J. Armstrong, "Experimental demonstrations of electronic dispersion compensation for long-haul transmission using direct-detection optical OFDM," *J. Lightw. Technol.*, vol. 26, no. 1, pp. 196–203, Jan. 2008.

[12] W. R. Peng, B. Zhang, K-.M. Feng, X. Wu, A. E. Willner, and S. Chi, "Spectrally efficient direct-detected OFDM transmission incorporating a tunable frequency gap and an iterative detection techniques," *J. Lightw. Technol.*, vol. 27, no. 24, pp. 5723–5735, Dec. 2009.

[13] Y. Zhang, M. O'Sullivan, and R. Hui, "Theoretical and experimental investigation of compatible SSB modulation for single channel long-distance optical OFDM transmission," *Opt. Exp.*, vol. 18, no. 16, pp. 16751–16764, 2010.

[14] V. Vujicic, P. M. Anandarajah, C. Browning, and L. P. Barry, "WDM-OFDM-PON based on compatible SSB technique using a mode locked comb source," *IEEE Photon. Technol. Lett.*, vol. 25, no. 21, pp. 2058–2061, Nov. 2013.

[15] M. S. Erkılınç, S. Kilmurray, R. Maher, M. Paskov, R. Bouziane, S. Pachnicke, H. Griesser, B. C. Thomsen, P. Bayvel, and R. I. Killey, "Dispersion-precompensated direct-detection Nyquist-pulse-shaped subcarrier modulation using a dual-drive Mach–Zehnder modulator," presented at the Optoelectronics Communications Conf., 2015.

[16] M. P. Thakur, M. C. R. Medeiros, P. Laurêncio, and J. E. Mitchell, "Optical frequency tripling with improved suppression and sideband selection," *Opt. Exp.*, vol. 19, no. 26, pp. B459–B470, 2011.

[17] A. Dochhan, H. Grieser, M. Eiselt, and J. P. Elbers, "Flexible bandwidth 448 Gb/s DMT transmission for next generation data center inter-Connects," presented at the European Conf. Optical Commun., Cannes, France, Paper P.4.10, 2014,

[18] R. I. Killey, P. M. Watts, M. Glick, and P. Bayvel, "Electronic dispersion compensation by signal predistortion using digital processing and a dual–drive Mach–Zehnder modulator," *IEEE Photon. Technol. Lett.*, vol. 17, no. 3, pp. 714–716, Mar. 2005.

[19] J. McNicol, K. Parsons, L. Strawczynski, and K. B. Roberts, "Electrical domain compensation of optical dispersion," presented at the Optical Fiber Commun. Conf., 2005, Paper OThJ3.

[20] D. McGhan, M. O'Sullivan, C. Bontu, and K. Roberts, "Electronic dispersion compensation," in *Proc. OFC*, tutorial, 2006.

[21] M. Seimetz, *High-Order Modulation for Optical Fiber Transmission*. New York, NY, USA: Springer-Verlag, pp. 18–21, 2009.

[22] K.-P. Ho and H.-W. Cuei, "Generation of arbitrary quadrature signals using one dual-drive modulator," *J. Lightw. Technol.*, vol. 23, no. 2, pp. 764–770, Feb. 2005.

[23] D. J. F. Barros and J. M. Kahn, "Optical modulator optimization for orthogonal frequency-division multiplexing," *J. Lightw. Technol.*, vol. 27, no. 13, pp. 2370–2378, Jul. 2009.

[24] V. Cizek, "Discrete Hilbert transform," *IEEE Trans. Audio Electroacoust.*, vol. 18, no. 4, pp. 340–343, Dec. 1970.

[25] O. O. Omomukuyo, "Orthogonal frequency division multiplexing for optical access networks," Ph.D. dissertation, Dept. Electron. Electr. Eng., Univ. Coll. London, London, U.K., 2013, pp. 47–55.

[26] M. Sieben, J. Conradi, and D. E. Dodds, "Optical single sideband transmission at 10 Gb/s using only electrical dispersion compensation," *J. Lightw. Technol.*, vol. 17, no. 10, pp. 1742–1749, Oct. 1999.

[27] G. P. Agrawal, *Applications of Nonlinear Fiber Optics*, 3rd ed. New York, NY, USA: Academic Press, 2010.

[28] C. E. Shannon, "A mathematical theory of communication," *Bell Syst. Tech. J.*, vol. 27, no. 3, pp. 379–423, 1948.

[29] R. A. Shafik, S. Rahman, and A. H. M. Islam, "On the extended relationships among EVM, BER and SNR as performance metrics," in *Proc. Int. Conf. Electr. Comput. Eng.*, 2006, pp. 408–411.

Authors' biographies not available at the time of publication.